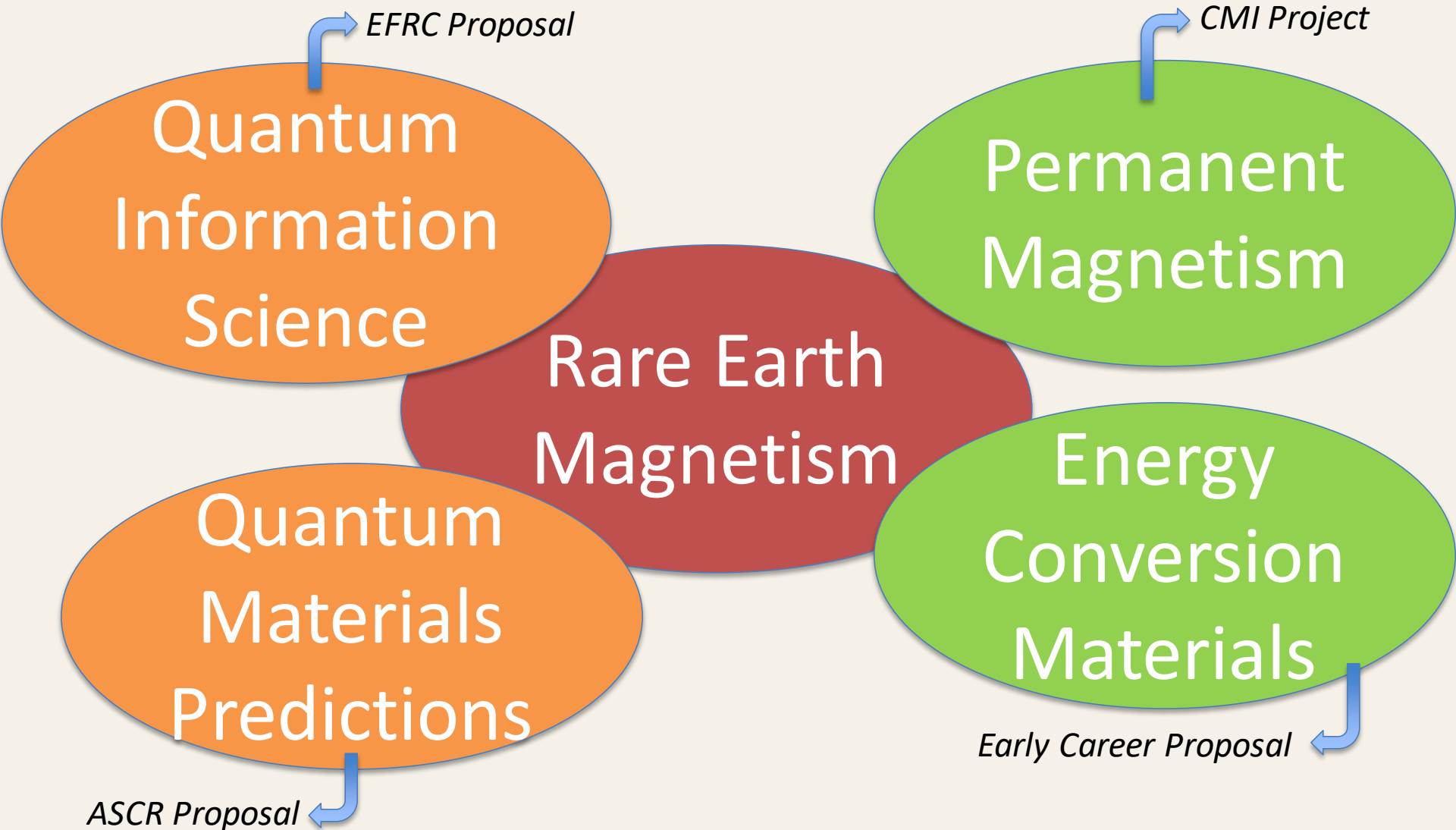


Symmetry and topology of rare-earth magnetic materials

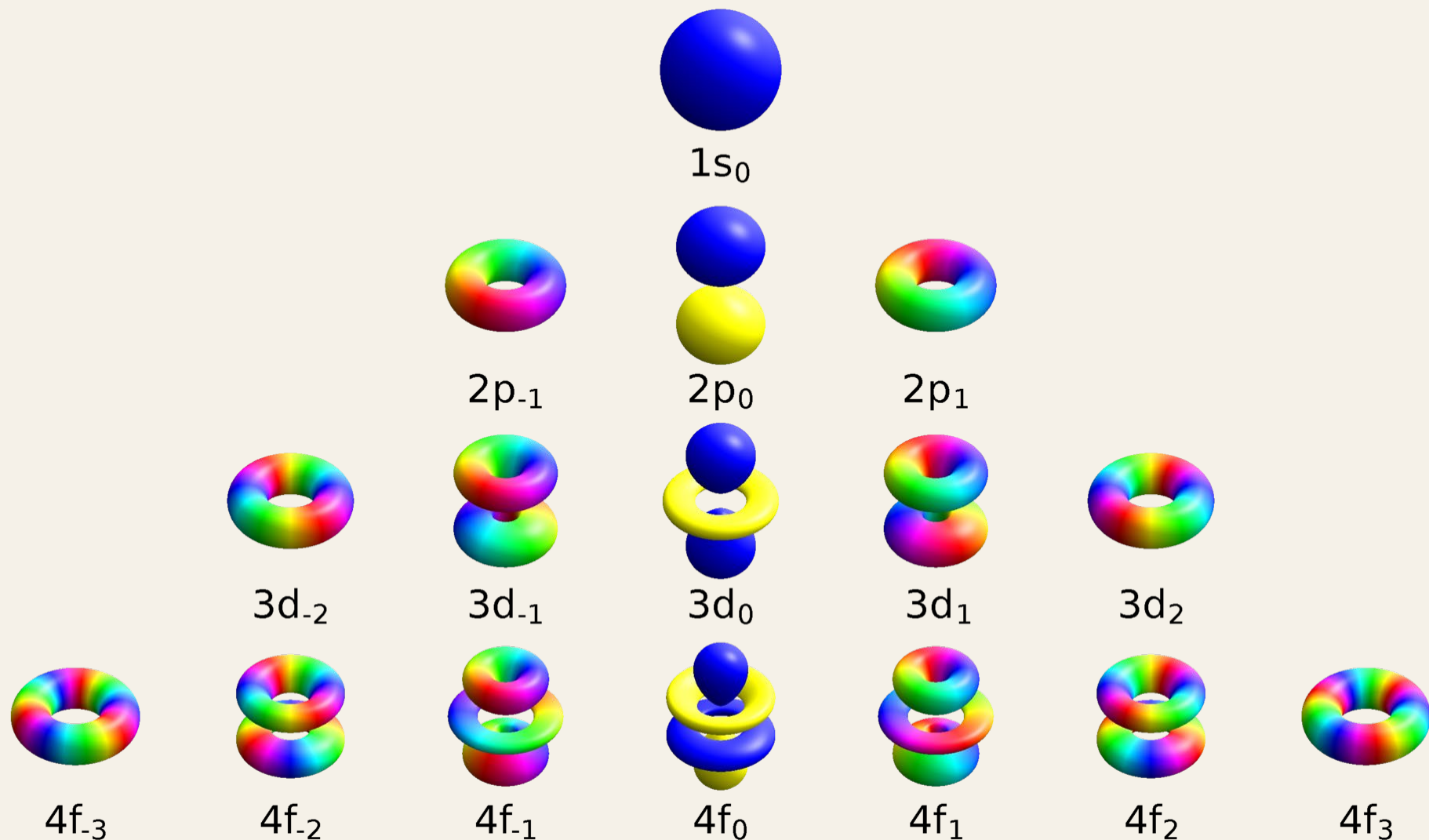
Durga Paudyal



Research Focus



Topology of Atomic Orbitals



Rare Earths

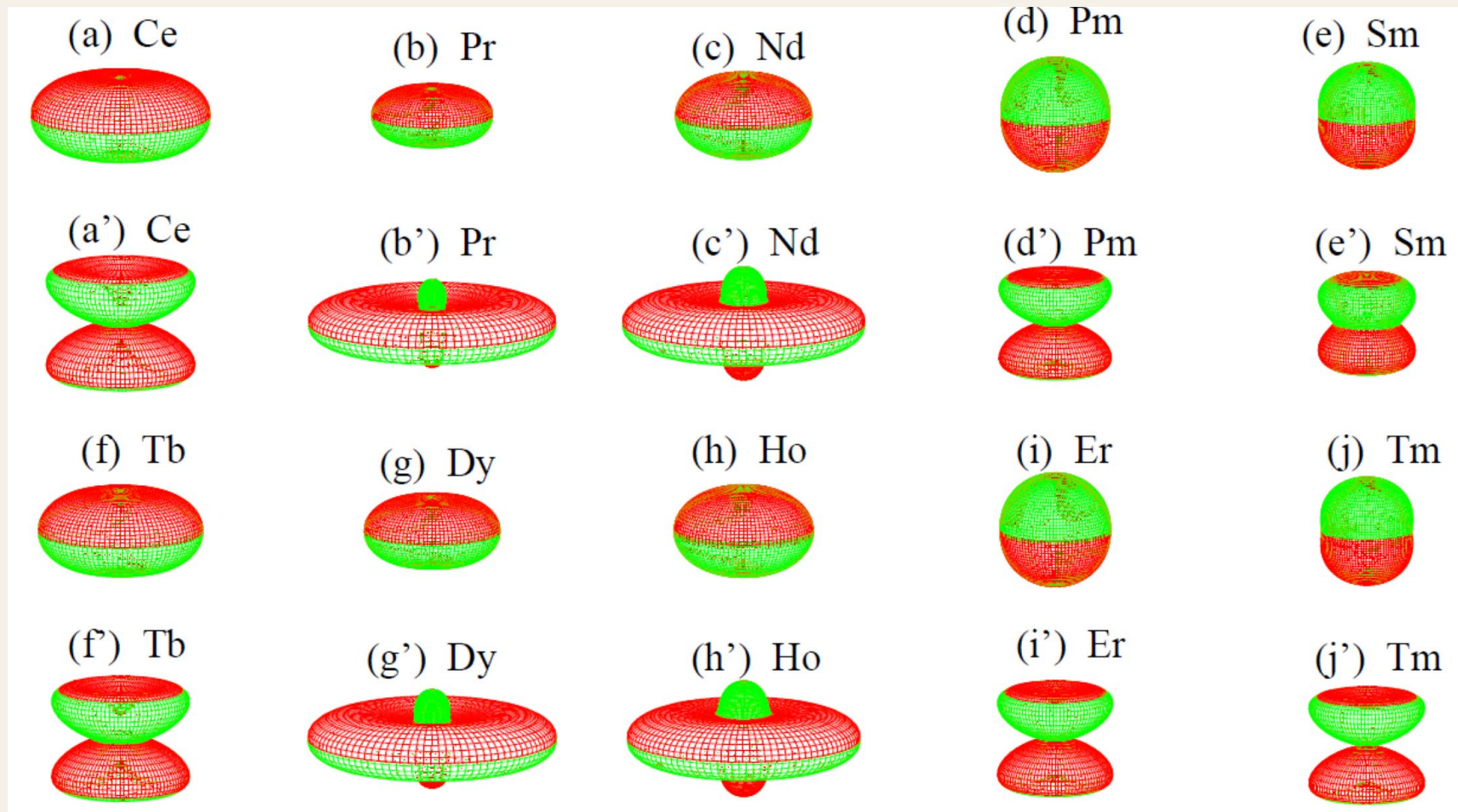
Electron Configurations in the Periodic Table

1 H 1s																	2 He 1s						
3 Li 2s	4 Be																	5 B 2p	6 C	7 N	8 O	9 F	10 Ne
11 Na 3s	12 Mg																	13 Al 3p	14 Si	15 P	16 S	17 Cl	18 Ar
19 K 4s	20 Ca	21 Sc	22 Ti	23 V	24 Cr	25 Mn	26 Fe	27 Co	28 Ni	29 Cu	30 Zn	31 Ga 4p	32 Ge	33 As	34 Se	35 Br	36 Kr						
37 Rb 5s	38 Sr	39 Y	40 Zr	41 Nb	42 Mo	43 Tc	44 Ru	45 Rh	46 Pd	47 Ag	48 Cd	49 In 5p	50 Sn	51 Sb	52 Te	53 I	54 Xe						
55 Cs 6s	56 Ba	57 La	72 Hf	73 Ta	74 W	75 Re	76 Os	77 Ir	78 Pt	79 Au	80 Hg	81 Tl 6p	82 Pb	83 Bi	84 Po	85 At	86 Rn						
87 Fr 7s	88 Ra	89 Ac	104 Rf	105 Db	106 Sg	107 Bh	108 Hs	109 Mt	110	111	112	113	114										
		58 Ce	59 Pr	60 Nd	61 Pm	62 Sm	63 Eu	64 Gd	65 Tb	66 Dy	67 Ho	68 Er	69 Tm	70 Yb	71 Lu								
		90 Th	91 Pa	92 U	93 Np	94 Pu	95 Am	96 Cm	97 Bk	98 Cf	99 Es	100 Fm	101 Md	102 No	103 Lr								



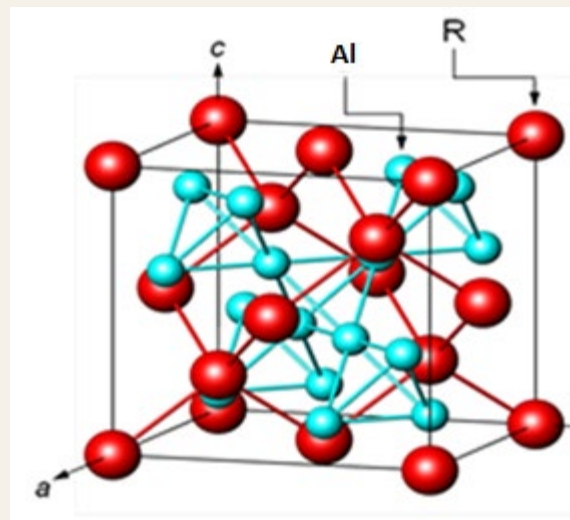
X = 1 to 14

Anisotropic Rare Earth Ions

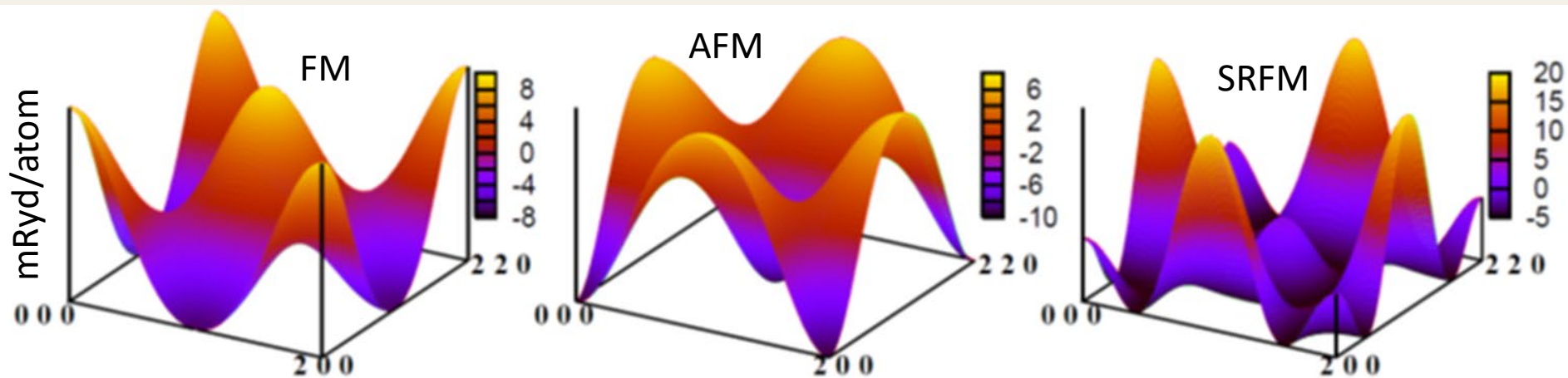


Short Range Ferromagnetism

Effective magnetic surface potentials calculated from density functional theory (DFT)



(Pr,Er)Al₂



PRB 2014, 2016

Density Functional Theory & Beyond

- ❑ The external potential (and hence the total energy), is a unique functional of the electron density
- ❑ The functional that delivers the ground state energy of the system gives the lowest energy if and only if the input density is the true ground state density
- ❑ Full potential to go beyond atomic sphere approximation
- ❑ Onsite electron correlation, **excited state, and dynamical mean field models** for more accurate description of occupied and unoccupied 4f states
- ❑ Spin orbit coupling to calculate direction dependent magnetic moments and magneto-crystalline anisotropy energy

Density Functional Theory & Beyond

Spin orbit coupling

$$\frac{1}{2m^2c^2r} \frac{dv}{dr} \mathbf{s} \cdot \mathbf{l}.$$

Crystal Field

$$v_{\text{cf}}(\mathbf{r}) = - \int \frac{e\rho(\mathbf{R})}{|\mathbf{r} - \mathbf{R}|} d\mathbf{R}$$

$$v_{\text{cf}}(\mathbf{r}) = \sum_{lm} A_l^m r^l Y_{lm}(\hat{\mathbf{r}})$$

Crystal field makes a contribution to the potential energy of a 4f electron

Density Functional Theory & Beyond

Magneto-crystalline anisotropy energy

Magnetocrystalline anisotropy energy (MAE) as the total energy difference with magnetic moment aligned along the planar and c-axis directions [$E_{hkl} - E_{001}$]

Anisotropic energy density relation

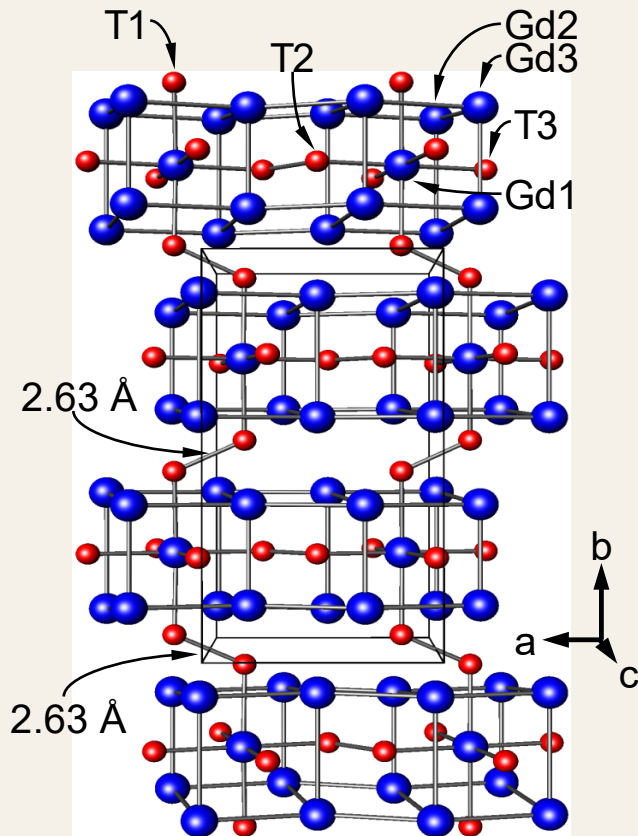
PRB 2017

$$\frac{E_a}{V} \approx \frac{\kappa_2}{2}(3\cos^2\theta - 1) + \frac{\kappa_4}{8}(35\cos^4\theta - 30\cos^2\theta + 3)$$

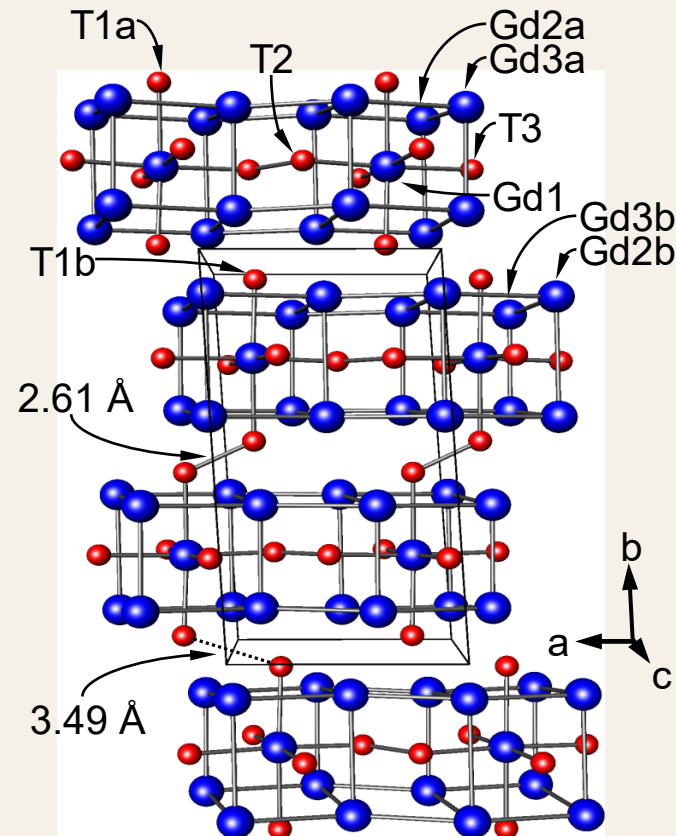
κ_2 (second-order) and κ_4 (fourth-order) coefficients are products of the corresponding quadrupolar/octupolar moments and crystal-field parameters

Energy Conversion Materials: Magnetocaloric Effect in $\text{Gd}_5\text{Si}_2\text{Ge}_2$

Orthorhombic below ~ 270 K



Monoclinic above ~ 270 K



PRB 2006

Magnetic exchange interactions and Curie temperature

- Heisenberg Hamiltonian with zero magnetic field

$$H = \sum_i \sum_{\delta} J_{i,i+\delta} \vec{S}_i \vec{S}_{i+\delta}$$

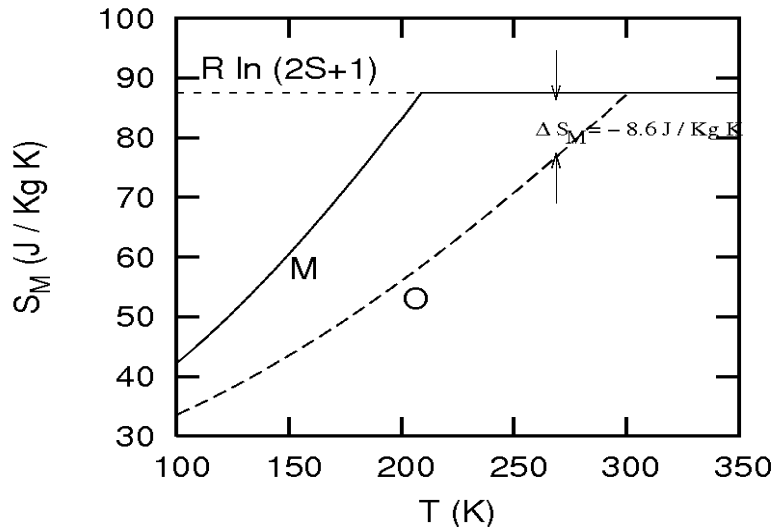
- Curie temperature in the mean field approximation

$$T_C = ZJ \frac{S(S+1)}{3k_B} = \frac{2}{3} \frac{E_{AFM} - E_{FM}}{k_B} = \frac{2}{3} \frac{J_O}{K_B}$$

Magnetic entropy change, magnetic free energy and magnetostructural transition in $Gd_5Si_2Ge_2$

Magnetic entropy

$$S_M \approx R \left[\ln(2J+1) - \frac{3}{2} \left(\frac{J}{J+1} \right) \sigma^2 - \frac{9}{20} \frac{(2J+1)^4 - 1}{[2(J+1)]^4} \sigma^4 \right]$$



At T_M , $U_1 - T_M S_1 = U_2 - T_M S_2$

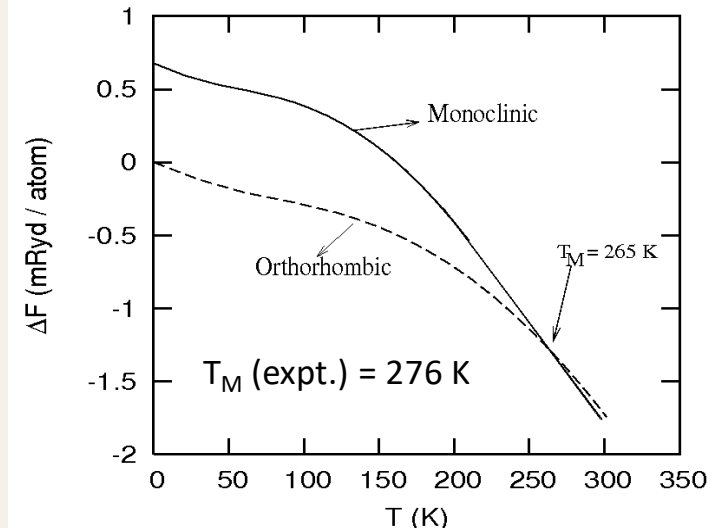
Magnetic entropy change $\Delta S_M = \frac{U_1 - U_2}{T_M}$

Magnetization

$$\sigma = \frac{M}{M_S} = \tanh \left[\frac{3J}{J+1} \frac{M}{M_S} \frac{T_C}{T} \right]$$

Magnetic free energy

$$F = -\frac{3}{2} \frac{J}{J+1} RT_C \sigma^2 - TS_M$$



Permanent Magnetism

With Post-Doc Renu Choudhary

Motivation

Prediction of new disruptive permanent magnetic materials that have high uniaxial magneto-crystalline anisotropy and magnetic moment with reduced critical elements

Goals and Objectives

Identify and employ novel methods to exploit 4f-elements for use in various novel rare earth element (REE) magnets

Theoretical assessment of optimal structural geometries to help accelerate the development of new materials with large magnetic anisotropies, moments, and magnetic transition temperatures

Anisotropy and quenched orbital moment in Sm-Co magnets

Achievement

Using electronic structure modeling, strong quenching of orbital magnetic moment was identified as the prime cause of unusually high magnetic anisotropy in SmCo_5

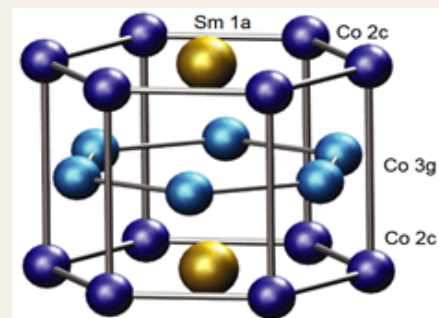
Significance and impact

- Demonstration of validated theory and modeling techniques to resolve unsolved key permanent magnet parameters such as magnetic anisotropy and orbital moment emerging from rare-earths
- Sm-Co magnets offer relatively high energy-product at high-temperature suitable for technological applications from electric vehicles to wind turbines

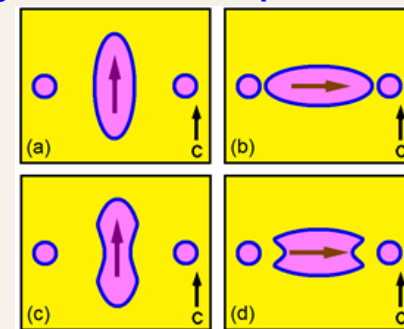
Details and next steps

- Electronic structure of the Sm atoms violates Hund's rules and the orbital moment is strongly quenched providing strong anisotropy and net 4f moment
- Rationalizing the orbital-moment quenching in terms of the dependence of the 4f charge distribution, a long-run future research will be necessary to reconcile experiment, sub-lattice model, and ab-initio theory

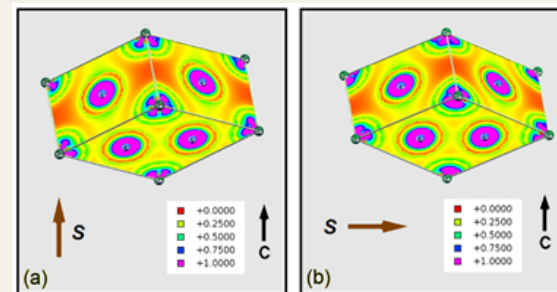
B. Das, R. Choudhary, R. Skomski, B. Balasubramanian, A. K. Pathak, D. Paudyal, and D. J. Sellmyer, Anisotropy and Orbital Moment in Sm-Co Permanent Magnets, *Phys. Rev. B* **100**, 024419 (2019).



Crystal structure of hexagonal SmCo_5 . Sm-1a, Co-2c, and Co-3g are three non-equivalent sites.

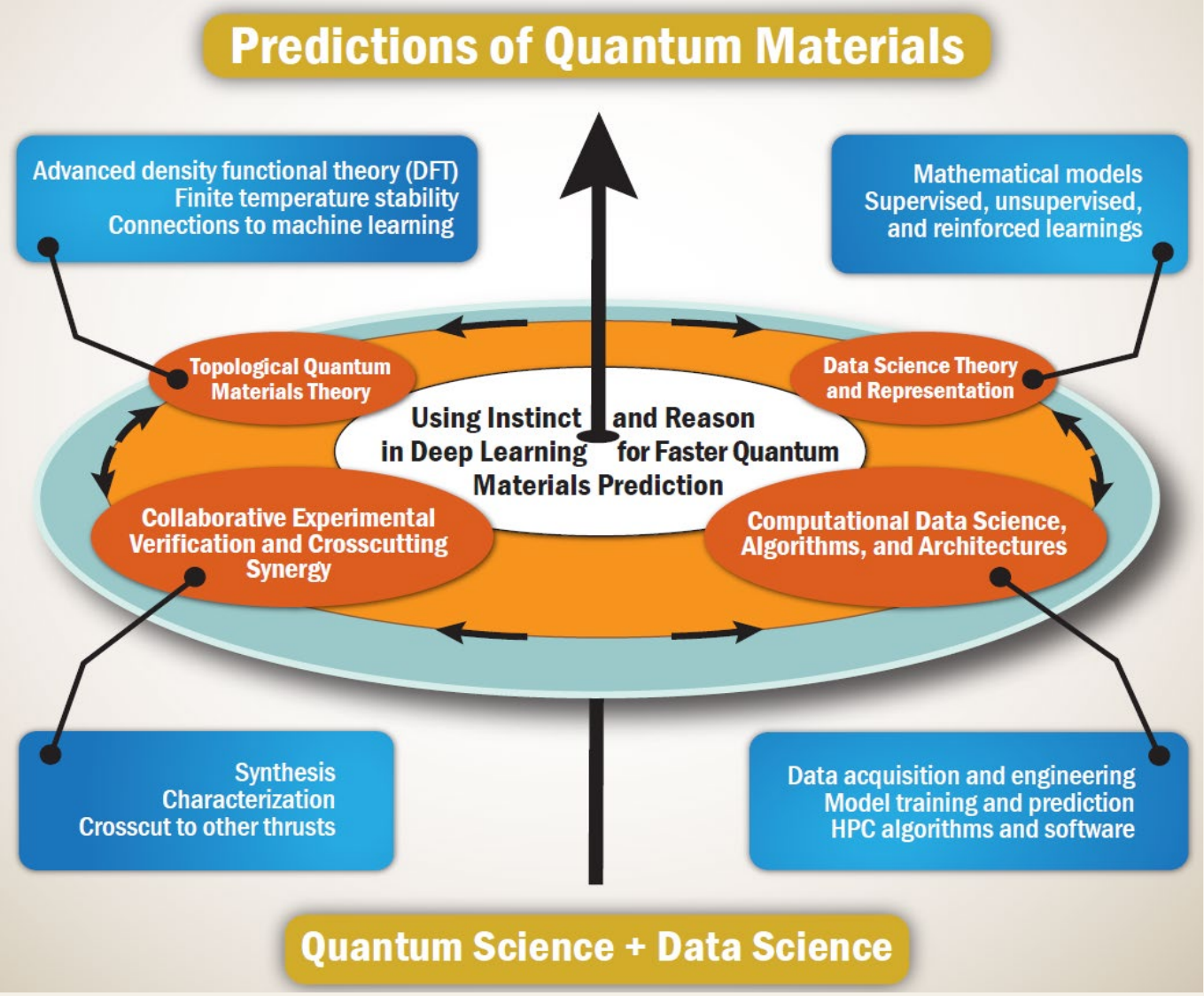


(a) and (b) charge distribution and rare-earth moment in the easy and hard directions, (c) and (d) effect of crystal field on the charge distribution for the easy and hard directions

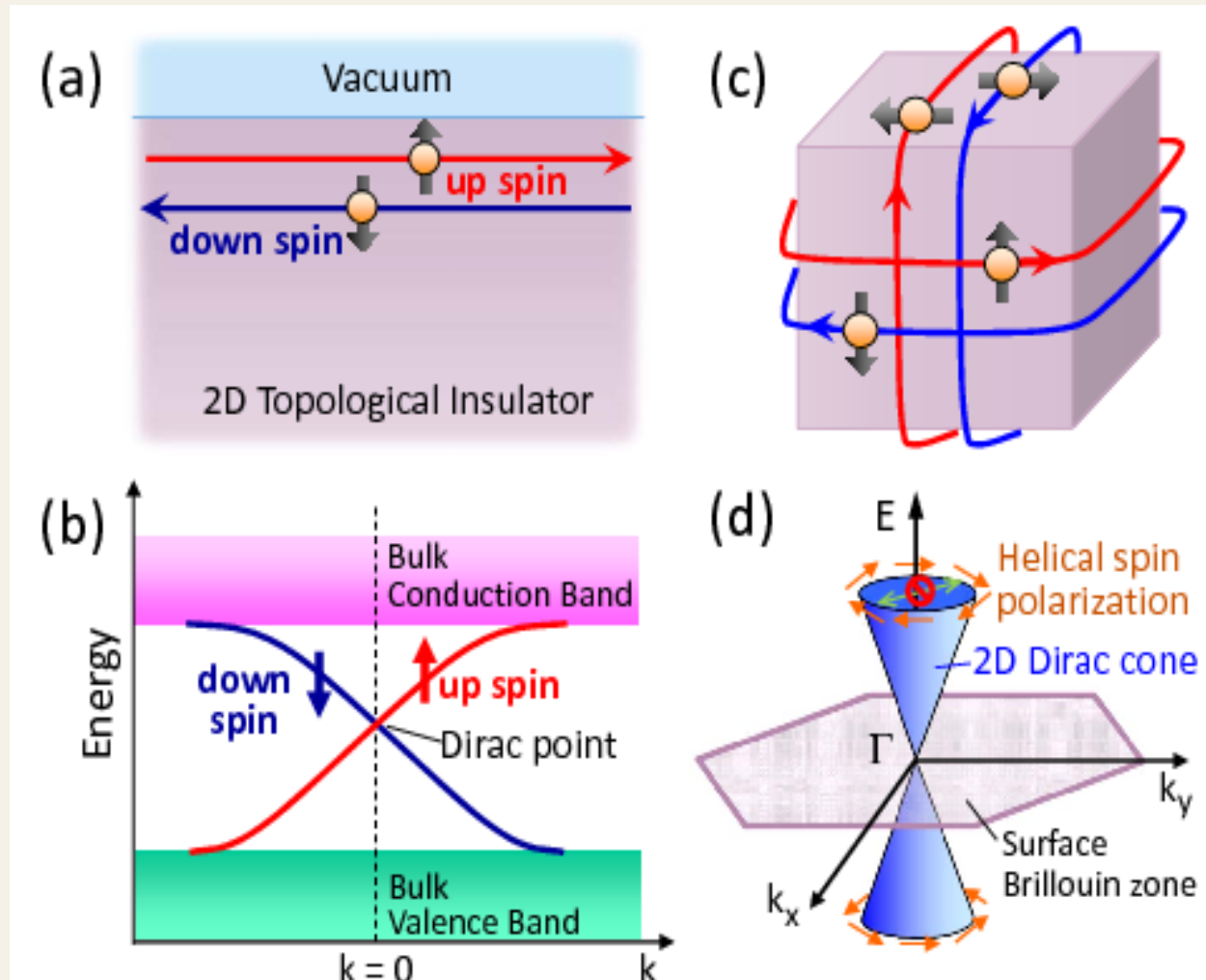


The charge density calculated employing density functional theory calculations

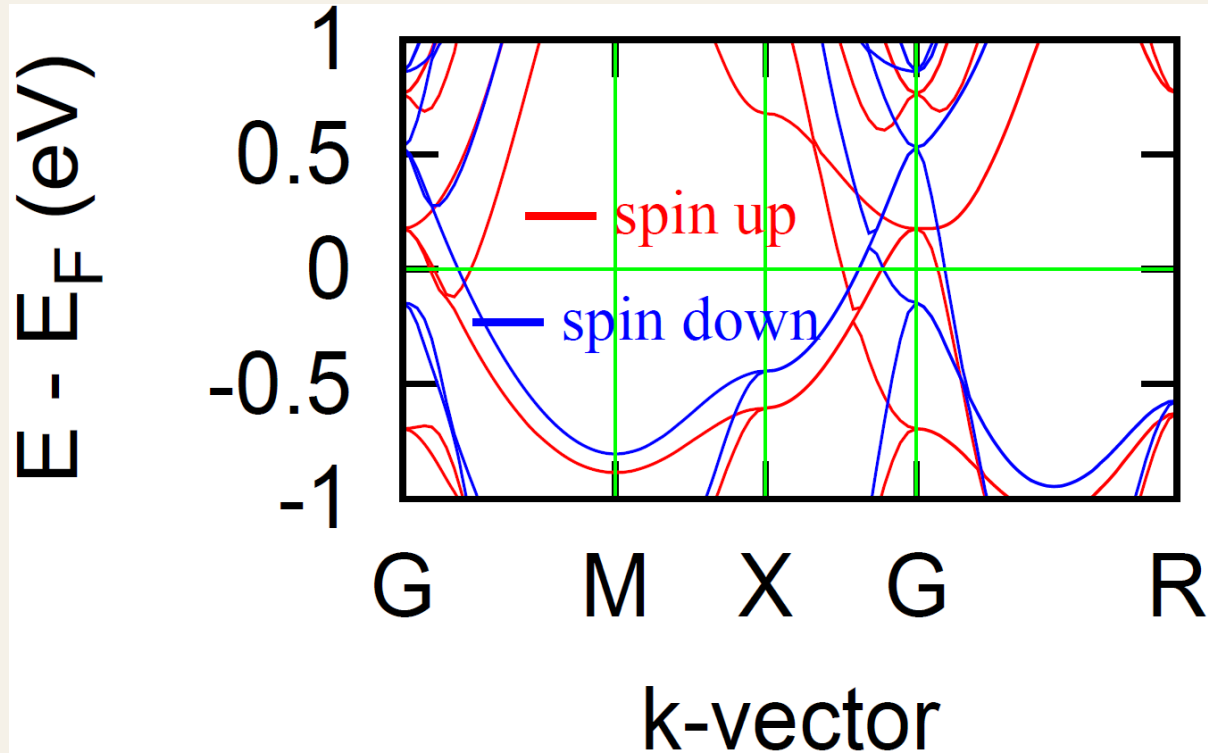
Quantum Materials Predictions



Quantum Materials Predictions

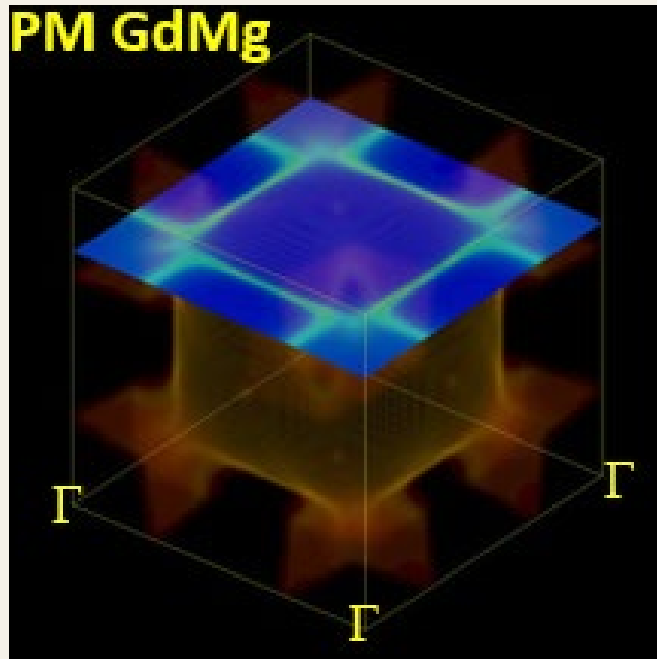


Quantum Materials Predictions

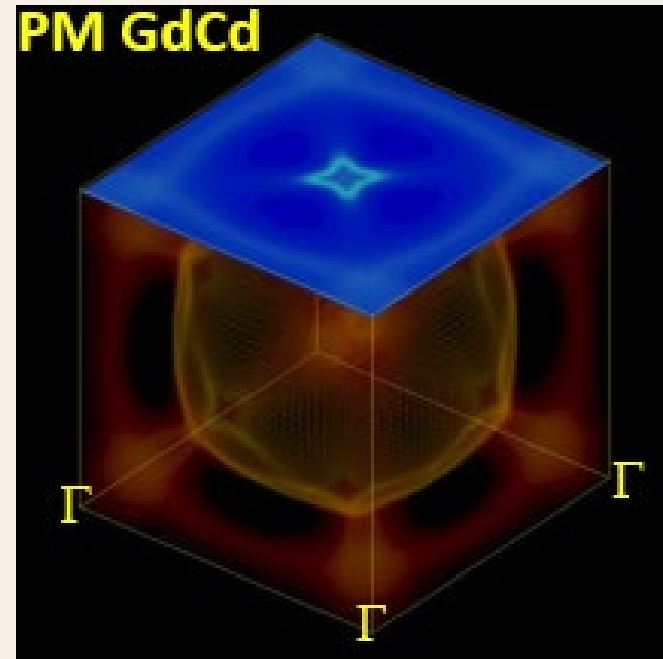


Complex band at the G (Γ) point and in the GX (Γ X) high-symmetry direction

Quantum Materials Predictions



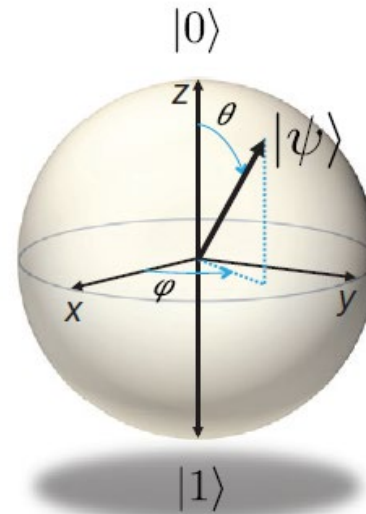
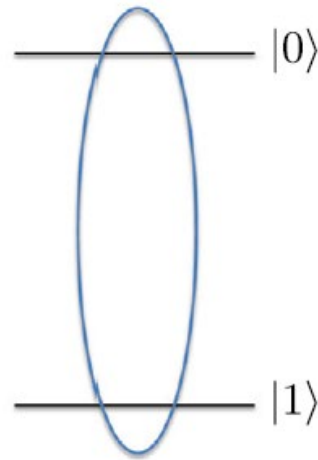
Wave vector $(0\ 0\ \frac{1}{2})$ nests large portions of parallel FS sheets, driving AFM correlations



A distinct topological transition – a hot spot formed around wave vector $(\frac{1}{2}\ \frac{1}{2}\ 0)$ when Mg is replaced by Cd, thereby suppressing the AFM and developing FM correlations

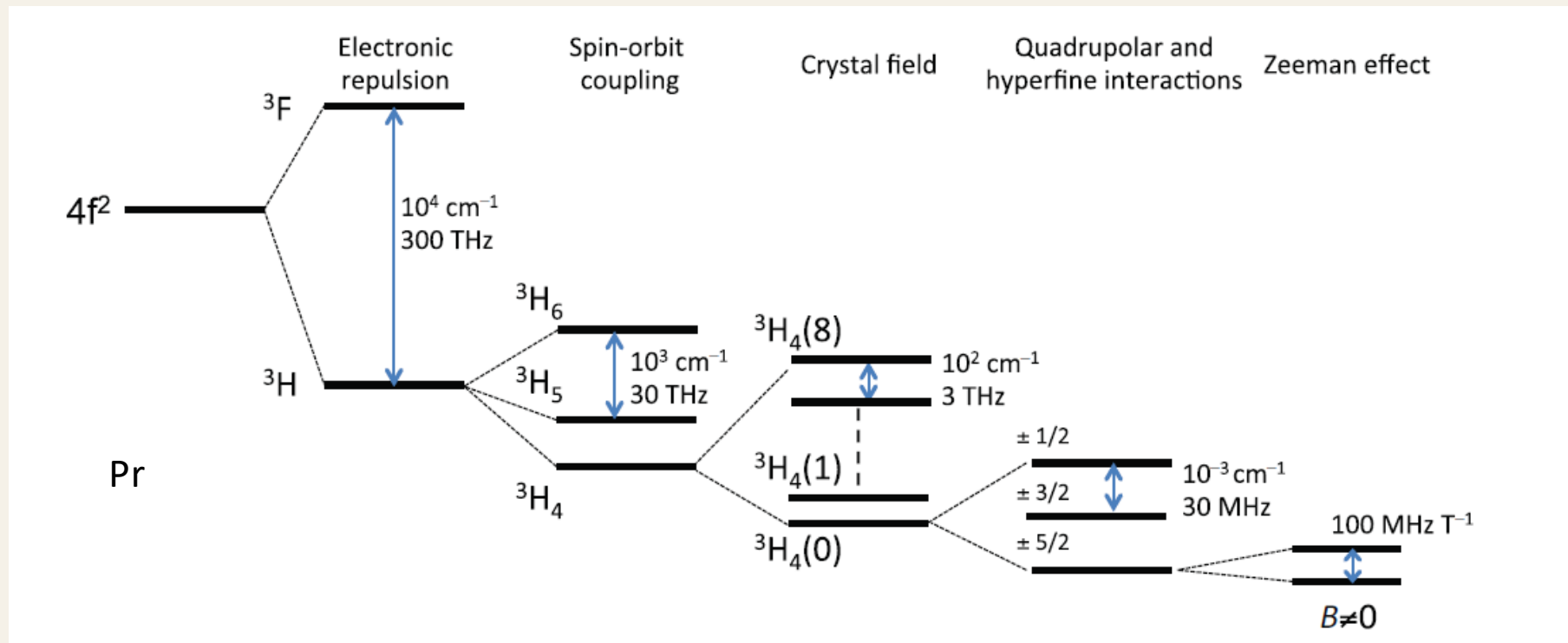
Quantum Information Science

$$|\psi\rangle = \cos(\theta/2)|0\rangle + e^{i\phi}\sin(\theta/2)|1\rangle$$



$$|\psi\rangle = \cos(\theta/2)|0\rangle + e^{i\phi}\sin(\theta/2)|1\rangle$$

Quantum Information Science



Interactions and partial energy-level scheme for Pr^{3+} ($I = 5/2$). The degeneracy of the hyperfine levels is lifted by an external magnetic field

Conclusion

Understanding of symmetry and topology will help build a foundation to discover quantum materials for current and future energy applications such as energy conversion, permanent magnet, and quantum information